

Synchrony and Clustering in Heterogeneous Networks with Global Coupling and Parameter Dispersion

Collins G. Assisi,¹ Viktor K. Jirsa,^{1,2} and J. A. Scott Kelso¹

¹Center for Complex Systems and Brain Sciences, Florida Atlantic University, Boca Raton, Florida 33431, USA

²Department of Physics, Florida Atlantic University, Boca Raton, Florida 33431, USA

(Received 5 May 2004; published 11 January 2005)

Networks with nonidentical nodes and global coupling may display a large variety of dynamic behaviors, such as phase clustered solutions, synchrony, and oscillator death. The network dynamics is a function of the parameter dispersion and may be captured by conventional mean field approaches if it is close to the completely synchronous state. In this Letter we introduce a novel method based on a mode decomposition in the parameter space, which provides a low-dimensional network description for more complex dynamic behaviors and captures the mean field approach as a special case. The example of globally coupled Fitzhugh-Nagumo neurons is discussed.

DOI: 10.1103/PhysRevLett.94.018106

PACS numbers: 87.18.Sn, 87.18.Hf, 87.23.Cc, 89.75.Hc

Low-dimensional dynamics in high-dimensional networks is a ubiquitous phenomenon observed in various physical, chemical, and biological problems [1–5]. In particular, networks with dispersed parameters may show such dynamics as a function of the parameter dispersion, including phase clustering and spatiotemporal quasiperiodic and chaotic dynamics [6]. Heterogeneous networks (that is, networks with parameter dispersion) with global coupling have been successfully described using a mean field approach [7] which relies on a local expansion around the synchronized solution. Here two sets of reduced equations are derived, in which the first describes the dynamics on the synchronization manifold and the second describes the deviations from synchrony. However, because the approach is valid only in the neighborhood of the synchronous solution, global network behaviors such as phase clustering cannot be described low dimensionally [8,9]. For instance, in the field of neuroscience, local populations of neurons are strongly connected within a small volume of cortical tissue and have been interpreted as the functional units of cortical processing [10]. These volume elements are described by a low-dimensional “effective” neuron [11], identical to the mean field, which will be legitimate only if the local network dynamics is synchronized. Otherwise, conditions are needed which, first, identify when the mean field dynamics fails and, second, provide alternative approaches to describe the low-dimensional network activity. The aim of our work is to obtain such a general formalism that may be used to approximate the effective dynamics of a high-dimensional heterogeneous network of globally coupled elements, which is not limited to synchronous behavior. We demonstrate that the collective behavior of globally coupled dynamical systems with parameter heterogeneity may be captured using a mode decomposition. These modes are defined in the space in which the parameter dispersion occurs and represent distinct patterns of collective behavior. Our approach success-

fully defines a low-dimensional approximation of the collective dynamics of the system, including various types of asynchronous behavior.

This Letter is organized into two parts. First, we consider a heterogeneous network of globally coupled excitable systems which are often used as toy models for neural behavior. We derive a set of mode equations that approximate its dynamics and, in the process, illustrate the core ideas of our approach. Second, we generalize our formalism to be applicable to networks with arbitrary dynamics at its nodes. One of the simplest examples of an excitable system is the Fitzhugh-Nagumo model [12]. Its variables, x and y , operate on slow and fast time scales, respectively. A globally coupled network of N Fitzhugh-Nagumo neurons is represented by the following equations:

$$\dot{x}_i = c \left(x_i - \frac{x_i^3}{3} + y_i \right) + K(X - x_i) + cz_i, \quad (1)$$

$$\dot{y}_i = \frac{1}{c}(x_i - by_i + a), \quad (2)$$

where $i = 1, \dots, N$ and K is the coupling strength. For an uncoupled network, $K = 0$. The intrinsic dynamics of the i th node is determined by the magnitude of the parameter, z_i , which may be interpreted as an external current or the degree of excitability of the neuronal membrane. For low values of z_i , the i th node has a stable fixed point. If a transient increase in z_i exceeds a threshold, the i th neuron performs a large excursion in the phase space before returning to a fixed point representing an action potential. Increasing z_i raises the cubic x nullcline, destabilizing the fixed point leading to a stable limit cycle (see Fig. 1). We introduce heterogeneity in the elements of the network by choosing the parameters z_i from a distribution $g(z)$ with mean μ_z and standard deviation σ . The average activity of the network, $X = \frac{1}{N} \sum_{i=1}^N x_i$, is used to drive each element, implying that every node is connected to every other node and the coupling strength between any two nodes is $\frac{K}{N}$. As a

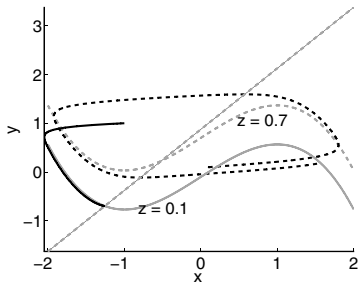


FIG. 1. The intrinsic dynamics of a node is illustrated. The nullclines are in gray. For low values of z_i (solid cubic nullcline), the trajectory (solid line) settles to a fixed point. Higher values of z_i (dashed cubic nullcline) lead to limit cycle oscillations (dashed trajectory).

function of K and the parameter dispersion, σ , we obtain different types of behavior, including a quiescent state [Fig. 2(a)], synchronous in-phase oscillations [Fig. 2(b)], and antiphase clustering [Fig. 2(d)]. In Fig. 2(c), some neurons perform subthreshold oscillations around a fixed point, while others perform suprathreshold oscillations. A characterization of the different types of collective behavior in the parameter space, K - σ , is shown in Fig. 3. Only positive values of K , for which antiphase clustering is not seen, are shown in the figure. Our numerical simulations show that, at each point in the $(K$ - $\sigma)$ space, the mean activity of the population, $X(t)$, is either quiescent or oscillatory. We define the amplitude of the mean field as the difference between the maximum and minimum values of $X(t)$ after the initial transients have settled. Figure 3 shows the contour lines of constant mean field amplitude. Three different regions of mean field dynamics are identified: (I) $K < 0.5$. Here, some of the neurons with low values of z perform subthreshold oscillations around a fixed point, while neurons with higher z values show phase

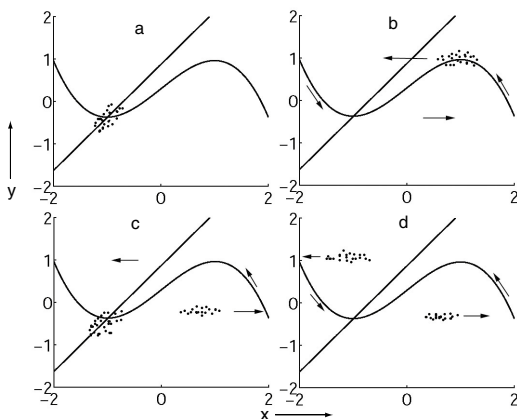


FIG. 2. Shown is a schematic of different scenarios for a population of coupled neurons in the phase space spanned by the variables x and y . Each dot represents the state of a neuron. (a) All the neurons settle to a fixed point. (b) The neurons oscillate in phase. (c) Some neurons perform subthreshold oscillations around a fixed point. Others oscillate along a limit cycle. (d) Antiphase clustering for $K < 0$.

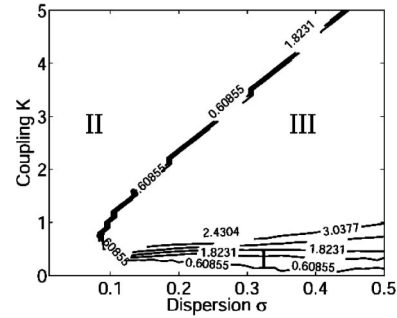


FIG. 3. This figure shows a contour map of the amplitude of the mean field calculated using 100 neurons for different values of the coupling strength K and the parameter dispersion σ . Only positive values of K are shown. See text for details.

locked suprathreshold oscillations. The dynamics in region I is shown in Figs. 2(c) and 4(c). (II) All the neurons settle to a fixed point. [Figs. 2(a) and 4(a)]. (III) The neurons perform suprathreshold synchronous oscillations [Figs. 2(b) and 4(b)]. A transition from region III to region II, mediated by an increase in the coupling strength, K , drives synchronously firing neurons to quiescence. For limit cycle oscillators with dispersed frequencies, this transition has been termed oscillator death [13]. An abrupt transition from region II to region III, fixed point behavior to synchronous in-phase oscillations, is mediated by an increase in the parameter dispersion, σ . Antiphase clustered solutions are obtained for $K < 0$. Stable phase clustered solutions have been demonstrated in systems of globally coupled inhibitory neurons [8,14] and Josephson junctions [9], and may be particularly relevant for neurobiological systems [3,4].

The core idea of our approach is the following: The dispersion of the parameter z_i creates an ordering of the nodes with regard to the magnitude of z_i ; that is, $z_{i+1} > z_i \forall i$. We indicate this parametric dependence in the notation of the state vector $q^i(t)$ of the i th node by writing $q^i(t) = (x_i(t), y_i(t))' = (q_1(z_i, t), q_2(z_i, t))'$ with the new vector components $q_k(z_i, t)$, $k = 1, 2$, $i = 1, \dots, N$, parametrized by z_i . The prime denotes the transposed vector.

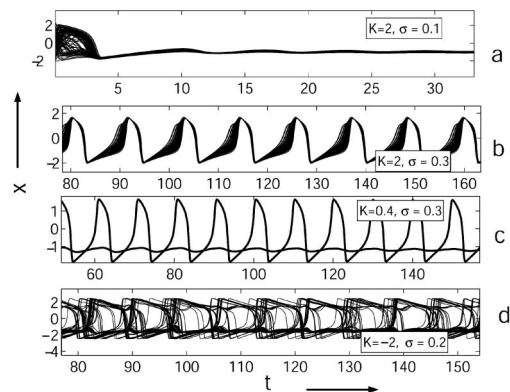


FIG. 4. The time series of a population of 100 neurons for various $(K$ - $\sigma)$ values.

In particular, if the number of neurons is sufficiently large, then it is justified to treat the set $\{z_i\}$, $i = 1, \dots, N$, as a continuous variable $z \in \text{Re}$ and the dispersed network state vector $q(t) = (\dots q_k(z_i, t) \dots) \rightarrow q(z, t)$ as a continuous vector field $q(z, t): \text{Re}^2 \rightarrow \text{Re}$ in the limit for large N . Then the mean field amplitude of the first component which couples the nodes is defined as

$$X(t) = \int_{-\infty}^{\infty} g(z) q_1(z, t) dz, \quad (3)$$

where the parameter, z , is distributed according to the function, $g(z)$. Equations (1) and (2) can now be rewritten as

$$\dot{q}_1(z, t) = c \left(q_1 - \frac{q_1^3}{3} - q_2 \right) + K[X - q_1] + cz, \quad (4)$$

$$\dot{q}_2(z, t) = \frac{1}{c} (q_1 - bq_2 + a). \quad (5)$$

Rewriting the network with heterogeneously distributed parameters as a vector field, $q(z, t)$, allows us to interpret the phenomena due to parameter dispersion as a spatio-temporal pattern formation process in z space. As a consequence, techniques become available which allow us to decompose the field $q(z, t)$ into its $m \leq N$ dominating patterns or modes $v_i(z)$ via

$$q(z, t) = \sum_{i=1}^m \begin{pmatrix} \xi_i(t) \\ \eta_i(t) \end{pmatrix} v_i(z) + R(z, t), \quad (6)$$

with their $2m$ time-dependent coefficients $\xi_i(t)$, $\eta_i(t)$. The remainder, $R(z, t)$, represents the spatiotemporal dynamics not captured by the m modes $v_i(z)$. Spatial mode decompositions are not unique and are biased towards certain criteria, such as the minimization of the square error (principal component analysis) or the statistical independence (independent component analysis). Other techniques utilize *a priori* knowledge about the system's dynamics to determine interpretable modes [15]. If the dispersion has multiple peaks in its distribution $g(z)$, then a separation of the peaks via a mode decomposition in z space is suggestive. The traditional mean field approach [7] is captured by the spatially uniform mode as a special case. In general, the modes will not be orthogonal, but an adjoint basis system $\{v_i^\dagger(z)\}$ can always be defined to guarantee biorthogonality:

$$\int_{-\infty}^{\infty} v_i^\dagger(z) v_j(z) dz = \delta_{ij}, \quad (7)$$

where δ_{ij} is the Kronecker symbol. If the normalized mean square error

$$E = \frac{\int_T \int_{-\infty}^{\infty} R(z, t)^2 dz dt}{\int_T \int_{-\infty}^{\infty} q(z, t)^2 dz dt} \quad (8)$$

is sufficiently small, then Eq. (6) may be truncated after the m th mode to obtain a low-dimensional description in terms of modes, $m \ll N$.

In our specific examples in Fig. 2, we choose the first two principal components, which are approximately non-overlapping rectangular modes, as the spatial modes $v_1(z)$, $v_2(z)$ motivated by the two different collective behaviors (subthreshold and suprathreshold oscillations). The temporal evolution of the coefficients of the i th mode, $(\xi_i(t), \eta_i(t))'$, is obtained by projecting Eqs. (4) and (5) onto the mode $v_i(z)$.

$$\dot{\xi}_i(t) = c \left(\xi_i - \epsilon_1 \frac{\xi_i^3}{3} - \eta_i \right) + K(A\xi_j - B\xi_i) + c\xi_i, \quad (9)$$

$$\dot{\eta}_i = \frac{1}{c} (\xi_i - b\eta_i + a\epsilon_2), \quad (10)$$

where $i, j = 1, 2$, $\epsilon_1 = \int_{-\infty}^{\infty} v_1(z)^4 dz$, $\epsilon_2 = \int_{-\infty}^{\infty} v_1(z) dz$, and $\xi_i = \int_{-\infty}^{\infty} z v_i(z) dz$. The cross terms resulting from the nonlinearities in Eq. (9) disappear because the modes $v_1(z)$ and $v_2(z)$ do not overlap. The constants A and B modulate the coupling between the modes and are given by

$$A_i = \int_{-\infty}^{\infty} g(z') v_i(z') dz' \cdot \int_{-\infty}^{\infty} v_i(z) dz - 1, \quad (11)$$

$$B_i = \int_{-\infty}^{\infty} g(z') v_j(z') dz' \cdot \int_{-\infty}^{\infty} v_i(z) dz. \quad (12)$$

Equations (9) and (10) define the reduced set of mode equations and represent a low-dimensional description of the dispersed network dynamics. These equations are similar to those of two coupled Fitzhugh-Nagumo neurons, justifying the approximation of the population mean activity by effective neurons as postulated by [10]. To test the reduced equations computationally, we choose the distribution function, $g(z)$, to be a Gaussian with standard deviation σ and solve the system numerically. Figure 5 describes the resulting different regimes of behavior in analogy to Fig. 3: (I) One mode, corresponding to lower values of z , shows subthreshold oscillations while the other mode shows suprathreshold oscillations. (II) Both modes settle to a fixed point. (III) The modes show synchronous in-phase oscillations. A comparison between Figs. 3 and 5

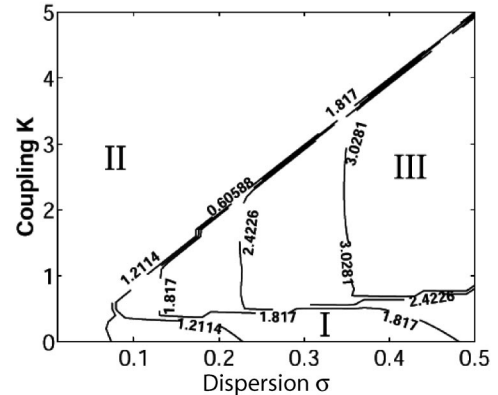


FIG. 5. This figure shows the contour lines of equal mean field amplitude in $(K-\sigma)$ space. The mean field is calculated from the low-dimensional mode description.

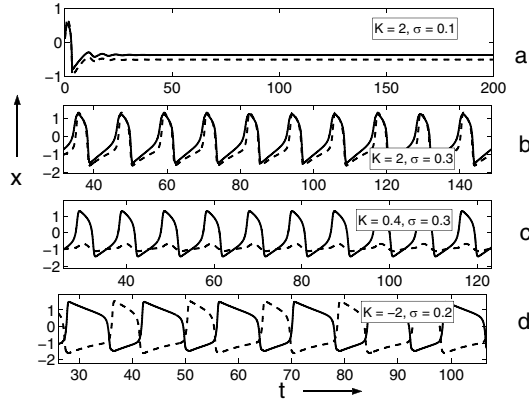


FIG. 6. The evolution of the time-dependent coefficients, $\xi_1(t)$ (dashed line) and $\xi_2(t)$ (solid line), is plotted for various $(K-\sigma)$ values as a function of time.

shows that our low-dimensional mode approximation provides a good description of the population behavior. A goodness of fit, $G = 1 - E$, [using Eq. (8)] is computed to be 86% for regime I, 99% for regime II, and 98% for regime III. The time series of the modes corresponding to each region in $K-\sigma$ space are shown in Figs. 6(a)–6(d).

We can now generalize this framework to a globally coupled network with arbitrary dynamical systems at its nodes. Consider a network of N elements given by the following equation:

$$\dot{\mathbf{x}}_i = f(\mathbf{x}_i, z_i) + \mathbf{K} \left[\frac{1}{N} \sum_{j=1}^N \mathbf{x}_j - \mathbf{x}_i \right], \quad (13)$$

where $\mathbf{x}_i = [x_i^{(1)} \cdots x_i^{(n)}] \in \text{Re}^n$ describes the n -dimensional dynamics of the i th node and $\mathbf{K} \in \text{Re}^n \times \text{Re}^n$ is a diagonal matrix with nonzero elements of the same value, K . The parameters, z_i , are dispersed according to the distribution function $g(z)$. In the new space defined by z , we introduce the vector field $\mathbf{q}(z, t) = [q_1(z, t) \cdots q_n(z, t)]$, where $q_j(z, t) = x_j^{(i)}(t)$, $j = 1, \dots, n$. Then, the corresponding dynamics can be written in terms of the new variable $q_j(z, t)$ as follows:

$$\dot{q}_j(z, t) = f_j(\mathbf{q}) + K \left[\int_{-\infty}^{\infty} q_j(z, t) g(z) dz - q_j(z, t) \right]. \quad (14)$$

Assume that the system can be described by a low-dimensional biorthogonal set of m modes in z space, $\{v_\ell(z), \ell = 1, \dots, m\}$, and its corresponding time-dependent coefficients, $[\xi_\ell^{(1)} \cdots \xi_\ell^{(n)}] \in \text{Re}^n$. Projecting Eq. (14) on each mode $v_\ell^\dagger(z)$, we obtain the following equations for the corresponding time-dependent amplitudes:

$$\dot{\xi}_\ell^j = h_\ell^j(\{\xi_k\}) + K [c_{v_\ell} (\xi_1^j g_{v_1} + \cdots + \xi_m^j g_{v_m}) - \xi_\ell^j], \quad (15)$$

where $h_\ell^j(\{\xi_k\}) = \int_z v_\ell^\dagger \cdot f_\ell^j(\mathbf{q}) dz$ depends on the set $\{\xi_k\}$, $g_{v_\ell} = \int_z v_\ell^\dagger \cdot g(z) dz$, and $c_{v_\ell} = \int_{-\infty}^{\infty} v_\ell^\dagger(z) dz$.

In summary, we have provided a low-dimensional description of a heterogeneous network of globally coupled dynamical systems. We demonstrated the existence of a phase transition from quiescent to synchronous oscillatory behavior mediated by parameter dispersion in a network of Fitzhugh-Nagumo neurons. The effects of parameter dispersion on neuronal systems may be particularly significant. An example can be found in CA1 stratum oriens interneurons in the hippocampus. Evidence from electrophysiological recordings show that hypothermia induced seizures in developing rats causes an increase in the variance of the resting membrane potential without causing a change in the mean resting potential [16]. One of the contributions of this Letter is to provide a method to describe phase clustering in networks of dynamical elements. The individual clusters are represented by distinct modes, and the interactions among these clusters may be described by the coupling between the mode equations. Further, our method does not assume a particular form of the parameter distribution function and is suitable to study networks with multimodal parameter distributions.

This work was supported by National Institute of Mental Health Grants No. MH 42900 and No. MH 01386.

-
- [1] Y. Kuramoto, *Chemical Oscillations, Waves and Turbulence* (Springer, Berlin, 1984).
 - [2] S. Nichols and K. Wiesenfeld, *Phys. Rev. A* **45**, 8430 (1992).
 - [3] A. K. Engel, P. Fries, and W. Singer, *Nat. Rev. Neurosci.* **2**, 704 (2001).
 - [4] J. A. S. Kelso, *Dynamic Patterns: The Self-Organization of Brain and Behavior* (MIT Press, Cambridge, MA, 1995).
 - [5] H. Haken, *Principles of Brain Functioning: A Synergetic Approach to Brain Activity, Behavior and Cognition*, Springer Series in Synergetics Vol. 67 (Springer, Berlin, 1996).
 - [6] P. C. Matthews and S. H. Strogatz, *Phys. Rev. Lett.* **65**, 1701 (1990).
 - [7] S. De Monte, F. d'Ovidio, and E. Mosekilde, *Phys. Rev. Lett.* **90**, 054102 (2003).
 - [8] J. Rubin and D. Terman, *J. Math. Biol.* **41**, 513 (2000).
 - [9] S. H. Strogatz and R. E. Mirollo, *Phys. Rev. E* **47**, 220 (1993).
 - [10] O. Sporns, J. A. Gally, G. N. Reeke, and G. M. Edelman, *Proc. Natl. Acad. Sci. U.S.A.* **86**, 7265 (1989).
 - [11] J. Buhmann, *Phys. Rev. A* **40**, 4145 (1989).
 - [12] R. Fitzhugh, *Biophys. J.* **1**, 445 (1961); J. Nagumo, S. Arimoto, and S. Yoshizawa, *Proc. IRE* **50**, 2061 (1962).
 - [13] Y. Yamaguchi and H. Shimizu, *Physica (Amsterdam)* **11D**, 212 (1984).
 - [14] D. Golomb, D. Hansel, B. Shraiman, and H. Sompolinsky, *Phys. Rev. A* **45**, 3516 (1992).
 - [15] C. D. Tesche, M. A. Uusitalo, R. J. Ilmoniemi, M. Huottilainen, M. Kajola, and O. Salonen, *Electroencephalogr. Clin. Neurophysiol.* **95**, 189 (1995).
 - [16] I. Aradi and I. Soltesz, *J. Physiol.* **538**, 227 (2002).